"Physics of Auroral Phenomena", Proc. XXXVI Annual Seminar, Apatity, pp. 106 - 109, 2013

Polar Geophysical Institute

COMMON FEATURES OF GLEs IN 19-24 SOLAR CYCLES

Yu.V. Balabin, E.V. Vashenyuk, B.B. Gvozdevsky, A.V. Germanenko *(Polar Geophysical institute, Apatity, Russia)*

Introduction

During strong solar flares the energetic particles are emitted into interplanetary space. Sometimes these particles reach the Earth and cause the events of ground level enhancement (GLE) of cosmic rays recorded by neutron monitors and sometimes even by muon telescopes. The worldwide NM network during its existence registered totally 71 ground level enhancements (GLEs). The first one was in 1942 and the last one was on 17 May 2012. Based on the data of the worldwide neutron monitor network it is possible to restore the primary spectrum of RSP by solving an inverse problem. It was done by many groups since the 70-ies of the XX century [1].

This paper presents our results of unified methodology processing of most of all GLEs. We have selected 51 events: from GLE05 (23.02.1956, 19th solar cycle) to GLE71 (17.05.2012, 24th solar cycle) suitable for modeling. The other events was either too weak or there was data from too few stations. Selected GLEs have a large range of increases from ~3% up to ~5000%. This amplitude threshold is necessary because the standard NM has accuracy of about 1.5% (as for five-minute data). For the selection and processing of these GLEs we used a unified method.

Technique of solving the inverse problem

The basis of the technique is a searching the RSP spectrum parameters which give the minimum difference between the calculated and measured response of NM. To calculate a NM response one have firstly to determine the asymptotic cone (AC) of acceptance for given station. AC refers to which direction the radiation arrives at the NM. In our work, AC is calculated for particles of 1 to 20 GV with a step 0.001 GV for all stations regardless of their cut-off rigidity. When calculating the AC for each station generates additional array of rigidities R, which indicating is this forbidden or allowed rigidity. This eliminates the problem of calculating the penumbra. When data about the state of the interplanetary medium are available, the magnetosphere model T01 is used. In other rare cases we used the T89 model. The calculation of AC is performed by the test particle technique. From the edge of the atmosphere (conditionally accepted height of 20 km) at the location of the station straight up a particle with rigidity R, mass of a proton and a negative charge (antiproton) is launched. Its path to escape from the Earth's magnetosphere is traced. Particle velocity vector outside the magnetosphere indicates the direction from which the proton with rigidity R must entry the magnetosphere to reach the NM station. If antiproton whith rigidity R can not get out of the magnetosphere, then the proton with rigidity R from outside the magnetosphere can not reach the station. Such rigidity is called forbidden for this station. Otherwise it is called allowed.

NM response to an isotropic flux of RSP is defined as:

$$\Delta N = \sum_{R=1}^{20} I(R) \cdot S(R) \cdot A(R) \cdot \Delta R \qquad (1)$$

where DN is a relative increase of the NM count rate; I(R) is a rigidity spectrum; S(R) is a Specific Yield Function (SYF) [2]; A(R)=1 for allowed rigidities and 0 for forbidden ones; DR is the rigidity step. SYF is a tabular value. Array A(R) is generated for each station in the calculation of the asymptotic cone. The general form of the specrum is

$$I(R) = J_0 \cdot R^{\gamma - \Delta\gamma(R-1)} \qquad (2)$$

where J_0 is an intensity of the flux at R=1 GV, g is a spectral index, Dg is a correction factor. Dg option provides variable slope of the spectral function. The three parameters of the spectral function (J0; g;Dg) are the values that uniquely determine it. They are energy parameters of the flux. Note especially that the spectral function takes no any particular form (power or exponential). However, for certain values of g and Dg it is possible to obtain a power law or an exponential form.

The real RSP flux is not isotropic. To take into account the anisotropy we take a basic pitch-angle distribution in the form of Gaussian:

$$G(\theta) = \exp(-\theta^2 / c) \qquad (3)$$

where c is a parameter characterizing the angle width of the flux, θ is the pitch angle of the particle with rigidity R, moving in the interplanetary magnetic field (IMF). To determine θ it is necessary to know the direction of the anisotropy axis. It can be defined by two angles λ and φ, latitude and longitude. So there are three parameters (c, λ and φ) describing RSP flux. They are spatial characteristics of RSP. As a result the expression (1) takes the form

$$\Delta N(J_0,\gamma,\Delta\gamma,c,\lambda,\varphi)=\sum_{R=1}^{20} I(R)\cdot S(R)\cdot A(R)\cdot G(\theta(R,\gamma,\varphi))\cdot \Delta R \qquad (4)$$

The discrepancy function, which must be minimized in the space of six parameters, is

$$\Phi(J_0,\gamma,\Delta\gamma,c,\lambda,\varphi)=\sum_{L}\left[\Delta N_L\cdot(J_0,\gamma,\Delta\gamma,c,\lambda,\varphi)-\Delta M_L\right]^2 \qquad (5)$$

where index L is the stations number, ΔM is actually observed increase at the station. The calculation of the minimum value of Φ provides the RSP flux parameters. More information about this technique can be found in [3, 4, 5].

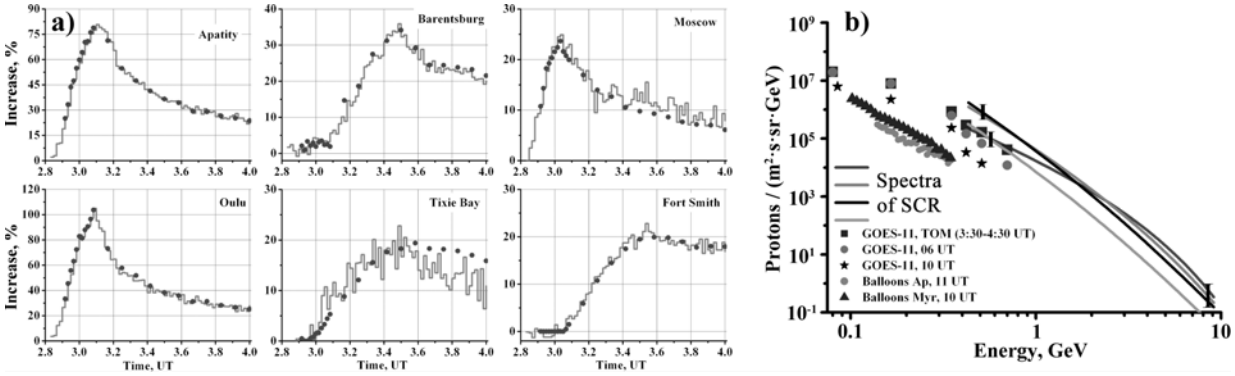

Fig. 1 GLE70. **a)** Increase profiles, experimental (solid lines) and derived (dots), of SCR at some stations. **b)** Derived spectra of SCR.

Function Φ in (5) is the baseline. In some cases the analysis of the profiles for events of increase using the data from the global network of stations, along with the interplanetary environment data indicates the presence of loop structures in the interplanetary magnetic field and the presence of the reverse (to the Sun) flux of RSP. Sometimes a detailed analysis of the amplitude distribution of increases in the global network of NM shows the intensity gap at pitch angles close to 90 degrees. In such cases the basic pitch angle distribution appears too coarse and the resulting solution has too big discrepancy. For such cases the function G(θ) was taken in the form considering features of RSP flux: bidirectional or with a depression at pitch angles close to 90 degrees. More about this see in [6].We note especially that in all these cases the modified form of function G(θ) for certain values of parameters converges monotonically to (3). This is done in order to minimize the error associated with a priori settings for solving the inverse problem.

Results

Totally about 50 events from GLE05 to GLE71 have been processed. The energy parameters of differential spectra are shown in the Table 1. While solving the inverse problem we used the rigidity values, and then translated results into the energy values in GeV. For all events shown in Table 1 calculation of the spectra was carried out at 5 minutes intervals. Thus it is possible to trace the dynamics of the spectra during the event. There are only three events for which there is no a five-minute data and the calculation of the spectra were done on hourly data. For short GLE (no longer than 3-4 hours) spectra were obtained from start to finish, for a long GLE spectra were calculated on the growth phase, the maximum and the start of the decreasing. The table demonstrates typical spectra of the growth/maximum phase and decrease phase for each event. For most events there are two components in the spectrum: prompt and delayed. Differential spectrum of the prompt component has an exponential form

$$I(E)=J_0\cdot\exp(-E/E_0) \qquad (6)$$

where J_0 is an intensity, proton/(m_2·s·sr·GeV); E_0 is a characteristic energy, GeV. The spectrum of the delayed component has a power law form

$$I(E)=J_1\cdot E^{-\gamma} \qquad (7)$$

where J_1 is an intensity at 1 GeV energy proton/(m_2·s·sr·GeV); g is a spectral index. Most of the spectra calculated by our technique are in good agreement with direct measurements in the stratosphere (80-400 MeV) and on spacecrafts (80-700 MeV).

Discussion

The list of studied events includes GLEs very different in amplitude, duration, and rigidity. There are both giant (GLE05, GLE69) and weak (GLE26, GLE40, GLE50) events. Events GLE05 and GLE42 are the most rigid; events GLE19 and GLE39 are very short, about half an hour. However, as the table shows, the most of GLE (~80%) consists of two components, called prompt and delayed. These components have different both energy and spatial parameters. The spectral function of the prompt component (PC) is exponential. The delayed component (DC) has a power law spectrum. The prompt component always has a high degree of anisotropy; the width of the flux does not exceed 60-70 degrees and at angles >90 the flux is completely absent. The delayed component is close to isotropic. On the growth phase (and at the maximumin in large events) RSP flux consists of PC. DC appears after the maximum and persists until the end of the event. The dynamics of the spectra (they are calculated in steps of 5 minutes) shows a smooth transition from one form of the spectrum to the other for 15-30 minutes. A small number of events consist of a single component. PC is absent in those GLE events which originate from the flare behind the Sun limb. Two events (GLE36 and GLE71) have no DC.

Table 1

GLE №	Inc. %	Prompt com		Delay com		GLE №	Inc. %	Prompt com		Delay com	
		J_0	E_0	J_1	-γ			J_0	E_0	J_1	-γ
05	5117	$7.4\cdot10^5$	1.37	$5.5\cdot10^5$	4.6	39	96	-	-	$5.2\cdot10^4$	5.9
08	253	$2.7\cdot10^5$	0.65	$1.6\cdot10^3$	4.2	40	6	$2.2\cdot10^2$	1.15	$5.8\cdot10^2$	4.4
10	144	-	-	$7.5\cdot10^3$	4.5*	41	15	$6.8\cdot10^3$	0.56	$3.8\cdot10^3$	5.1
11	111	-	-	$1.0\cdot10^5$	5.3	42	392	$1.5\cdot10^4$	1.74	$2.5\cdot10^4$	4.1
13	18	$5.2\cdot10^3$	0.52	$3.6\cdot10^3$	6.0	43	49	$4.0\cdot10^4$	0.53	$3.0\cdot10^4$	4.8
16	19	$1.4\cdot10^4$	0.58	$6.7\cdot10^3$	4.7	44	154	$7.5\cdot10^4$	0.91	$1.5\cdot10^4$	6.1
19	12	$1.2\cdot10^4$	0.58	$2.6\cdot10^3$	5.5	45	114	$2.4\cdot10^4$	0.72	$1.1\cdot10^5$	4.9
20	15	$6.2\cdot10^4$	0.47	$4.6\cdot10^3$	5.1	46	23	$6.3\cdot10^3$	1.13	$2.7\cdot10^3$	4.3
21	7	-	-	$7.4\cdot10^2$	4.4*	48	43	$2.8\cdot10^4$	0.60	$9.1\cdot10^3$	4.3
22	28	$3.4\cdot10^4$	0.45	$8.7\cdot10^3$	5.8	49	8	-	-	$9.0\cdot10^3$	4.7
23	12	-	-	$3.7\cdot10^3$	5.1**	51	8	$2.6\cdot10^3$	0.83	$3.3\cdot10^3$	4.8
24	36	-	-	$1.5\cdot10^3$	7.1	52	26	-	-	$5.8\cdot10^3$	4.6
25	8	$6.6\cdot10^2$	1.23	$4.3\cdot10^2$	5.0	55	11	$8.3\cdot10^3$	0.92	$8.2\cdot10^3$	4.6
26	5	$3.7\cdot10^3$	0.51	-	-	59	40	$3.3\cdot10^5$	0.50	$5.0\cdot10^4$	5.4
27	13	$6.6\cdot10^5$	0.32	$6.7\cdot10^3$	5.7	60	123	$1.3\cdot10^5$	0.62	$3.5\cdot10^4$	5.3
28	4	$2.2\cdot10^4$	0.48	$3.3\cdot10^2$	4.8	61	15	$2.5\cdot10^4$	0.52	$1.2\cdot10^3$	3.6
29	9	$6.5\cdot10^2$	1.14	$9.3\cdot10^2$	3.2	65	43	$1.2\cdot10^4$	0.60	$1.5\cdot10^4$	4.4
30	33	$1.5\cdot10^4$	0.77	$1.1\cdot10^4$	4.7	67	16	$4.6\cdot10^4$	0.51	$9.7\cdot10^3$	6.3
31	208	$3.5\cdot10^4$	1.11	$1.3\cdot10^4$	4.0	69	2751	$2.5\cdot10^6$	0.49	$7.2\cdot10^4$	5.6
32	8	$1.5\cdot10^4$	0.41	$7.0\cdot10^2$	4.7	70	93	$3.5\cdot10^4$	0.59***	$4.3\cdot10^4$	5.7
36	9	$4.5\cdot10^4$	1.21	-	-	71	18	$1.5\cdot10^5$	0.34	-	-
38	54	$5.7\cdot10^3$	0.65	$7.2\cdot10^3$	4.5						

* - from hourly data
** - approximation, real spectrum isn't pure power law
*** - approx., real spectrum isn't pure exponent

The exponential spectrum shape of the PC indicates that the particles of this flux were accelerated in an electric field. Only this type of acceleration gives such spectrum. Electric fields can be generated during magnetic reconnection in the active region on the Sun. For more details see [7, 8]. PC particles are emitted immediately from the Sun along the open field lines and reach the Earth first.

The Fig. 2 shows the spectra of PC and DC of all the events listed in the table. DC spectra clearly grouped into two subsets. The first set has a hard spectrum with a value of $g \sim 4$, the second one has a soft spectrum with $g \sim 6$. PC spectra are located different. Most of the spectra are in a group that has the characteristic energy $E_0 \sim 0.45$–0.65 GeV. Spectra with the value of $E_0 > 0.9$ GeV are in a small scattered group. It includes PC spectra of outstanding events GLE05, GLE42, GLE69. In our previous work [9] it was found that, due to specific NM sensitivity huge NM increase can be produced at low intensity J_0 of PC. To produce ~1000% NM increase, DC should have intensity J_1 around two magnitude orders higher than usual, but direct measurements in the stratosphere and on the spacecrafts do not reveal such intensity.

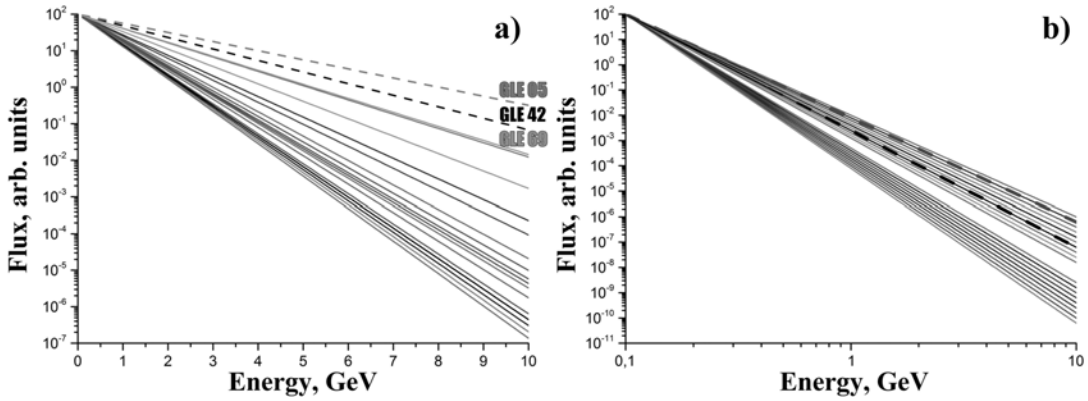

Fig. 2 The spectra of prompt (a) and delayed (b) components. For readability the spectra are normalized to highlight their important characteristic - the slope. The PC spectra of the GLE05, GLE42, GLE69 events are outstanding in their hardness. DC spectra for these events are not different from the others.

Conclusions

Available in three out of for dozens of GLE events with two components argues that the presence of the PC in the growth phase and the DC after the maximum is typical. However, the exponential spectrum can only be produced by acceleration of charged particles in electric fields. With high certainty it can be argued that during flares in the active regions on the Sun electric fields are present and we see their results as PC.

Explanation of the large GLE events was given. According measurements in the stratosphere and on spacecrafts, these events are not outstanding. Large increases are explained by specific NM sensitivity: NM response on the flux with the exponential spectrum is much more than a flux with a power spectrum.

Acknowledgments. This work was supported by the RFBR grant 12-02-01305-a.

References

1. M.A. Shea, D.F. Smart, Space Sci. Rev. 32 (1982) 251-255.
2. H. Debrunner, E. Flueckiger, J.A. Lockwood, 8th European Cosmic Ray Symposium Book of Abstracts (1984).
3. L.I. Miroshnichenko et. al:, Journal of Geophysical Research 110 (2005) a09s08 doi:10.1029/2004ja010936.
4. J. Perez-Peraza, E.V. Vashenyuk, L.I. Miroshnichenko, Yu.V. Balabin, A. Gallegos-Cruz, The Astrophysical Journal 695 (2009) 865873.
5. E.V. Vashenyuk, Yu.V. Balabin, B.B. Gvozdevsky, L.I. Shchur, Geomagnetism and Aeronomy 48 (2008) 149153.
6. J.A. Perez-Peraza, E.V. Vashenyuk, A. Gallegos-Cruz, Y.V. Balabin, L.I. Miroshnichenko, Advances in Space Research 41 (2008) 947954.
7. Yu.V. Balabin, E.V. Vashenyuk, O.V. Mingalev, A.I. Podgorny, I.M. Podgorny, Astronomy Reports 49 (2005) 837846.
8. I.M. Podgorny, Yu.V. Balabin, E.V. Vashenyuk, A.I. Podgorny, Bulletin of the Russian Academy of Sciences. Physics 75 (2011) 738-740.
9. E.V. Vashenyuk, L.I. Miroshnichenko, . Perez-Peraza, Yu.V. Balabin, B.B. Gvozdevsky, A. Gallegos-Cruz, Proc. of 30 ICRC (2007).